Mon. Not. R. Astron. Soc. **000**, 000–000 (0000) Printed 5 February 2008 (MN LATEX style file v2.2)

Halo evolution in the presence of a disc bar

Paul J. McMillan and Walter Dehnen
Department of Physics & Astronomy, University of Leicester, Leicester, LE1 7RH

5 February 2008

ABSTRACT

Angular momentum transfer from a rotating stellar bar has been proposed by Weinberg & Katz (2002) as a mechanism to destroy dark-matter cusps in a few rotation periods. The *N*-body simulations performed by these authors in support of their claim employed spherical harmonics for the force computation and were, as shown by Sellwood (2003), very sensitive to inclusion of asymmetric terms (odd l, m). In order to disentangle possible numerical artifacts due to the usage of spherical harmonics from genuine stellar dynamical effects, we performed similar experiments using a tree code and find that significant cusp destruction requires substantially more angular momentum than is realistically available. However, we find that the simplified model (a *N*-body halo torqued by a rotating bar pinned to the origin) undergoes an instability in which the cusp moves away from the origin. In presence of this off-centring, spherical density profiles centred on the origin display an apparent cusp-removal. We strongly suspect that it is this effect which Weinberg & Katz observed. When suppressing the artificial instability, cusp removal is very slow and requires much more angular momentum to be transferred to the halo than a realistic stellar bar possibly possesses.

Key words: Methods: *N*-body simulations – Galaxies: kinematics and dynamics – Galaxies: evolution – dark matter

1 INTRODUCTION

Cold Dark Matter (CDM) cosmological simulations consistently predict that the density profile of dark matter halos increases sharply towards the centre, creating a 'cusp', where the density increases like a inverse power-law. Navarro, Frenk & White (1996) proposed

$$\rho(r) = \frac{\rho_c}{(r/r_s)(1 + r/r_s)^2}, \quad (1)$$

as a universal density profile (hereafter called 'NFW') for CDM haloes of all masses. Here, r_s is a scale radius and ρ_c is a characteristic density. This density profile has a central slope of $\mathrm{d}\ln\rho/\mathrm{d}\ln r = -1$. Later work has questioned this inner slope and the universality over all halo masses, but the existence of a cusp with $\mathrm{d}\ln\rho/\mathrm{d}\ln r$ in the range -1 to -1.5 is a robust prediction of such simulations (e.g. Moore et al. 1998; Power et al. 2003).

Observations of the rotation curves of disk galaxies are the best probes of dark matter on galactic scales, and while some studies cannot rule out consistency with a cuspy NFW-like profile (Swaters et al. 2003; van den Bosch & Swaters 2001), the majority of the observations are claimed to be inconsistent with the density profile model (Côté et al. 2000; Binney & Evans 2001; de Blok et al. 2001a,b; Blais-Ouellette et al. 2001; Salucci et al. 2003; Gentile et al. 2004). Investigations combining rotation curves with gravitational lensing observations came to the same conclusion (Trott & Webster 2002). While it has been suggested that the discrepancy may be a result of direct comparison with the NFW fitting formula, rather than with more realistic triaxial halos (Hayashi et al. 2004), it is considered the greatest current challenge of the CDM paradigm.

Numerous possibilities have been put forward in an effort to explain the difference between theory and observation. Many of these involve altering the assumed properties of dark matter, either the dark matter particle itself (Spergel & Steinhardt 2000; Kaplinghat et al. 2000), or the initial power spectrum on small scales (warm dark matter; e.g. Colín et al. 2000; Bode et al. 2001). Since the central region of most galaxies are dominated by baryonic matter, it seems reasonable that the interaction between baryonic and dark matter will have a major effect upon the dark matter density in the inner region of the halo. If the effect of this interaction was to reduce the dark matter density at the centre of the halo, then this could potentially solve the problem. Several investigation of such processes have been undertaken, some pointing out effects that would *increase* the gradient of the density cusp still further (Blumenthal et al. 1986), some discussing processes that could potentially remove the cusp (Binney et al. 2001; El-Zant et al. 2001; Weinberg & Katz 2002). In this paper we investigate the mechanism proposed by Weinberg & Katz, of angular momentum transfer from a rotating disc bar to the halo as a means of removing a cusp.

Weinberg & Katz pointed to an earlier study by Hernquist & Weinberg (1992) to suggest that angular momentum would be rapidly transfered from a rotating disc bar to the halo at an inner Lindblad-like resonance. Weinberg & Katz supported the hypothesis with analytical calculations and simplified *N*-body simulations. In the simulations, the gravitational potential of a

rotating bar, with centre pinned at the initial centre of the density distribution, was imposed upon an N-body representation of a CDM halo with an NFW profile.

The simulations of Weinberg & Katz were re-examined by Sellwood (2003) who found the same reduction in central density, but argued that the deliberately artificial perturbation applied to the system lead to misleading results. Sellwood (2003) ran fully self-consistent simulations, which showed a slight *steepening* of the halo's inner profile from the action of a bar. This result was also seen in the simulations of Valenzuela & Klypin (2003). However the self consistent simulations of Holley-Bockelmann et al. (2003) showed a clear flattening in the cusp, as do the later ones of Weinberg (2004). A discussion of this apparently irreconcilable discrepancy was given by Athanassoula (2004).

The simulations of Weinberg & Katz (2002) and Sellwood (2003), and also the original study of Hernquist & Weinberg (1992) all employed spherical harmonics to compute the gravitational potential and accelerations. The main motivation for this choice was the high symmetry of the problem, which allows the restriction to a low number of harmonics. This in turn reduces the computational effort and enables a larger number N of bodies and hence higher numerical resolution than with more traditional methods, such as the Barnes & Hut (1986) tree code. In fact, Weinberg & Katz (2002) even claim that cusp removal cannot be successfully simulated by a tree code (unless $N \gg 10^6$), because the noise in the forces would scatter bodies off the resonant orbits, which, according to these authors, are driving the angular momentum transfer. Because of this argument, it was not entirely clear whether the aforementioned results of fully self-consistent simulations are realistic or not.

There is, however, a price to pay for using spherical harmonics. Most importantly, any method based on spherical polar coordinates is vulnerable to off-centring: if the modelled density distribution is not centred on the origin of the coordinate system, many terms are required for the series to converge. Conversely, when off-centring occurs, the gravity obtained from only the first few terms is strongly biased, which may induce artificial $m = 1$ instabilities and/or interfere with natural $m = 1$ instabilities. The only proper way to avoid this problem is to enforce centring, i.e. not allowing coefficients with odd l, m to carry any weight. Clearly, this makes systems with any properties that are not reflection symmetric, including instabilities, impossible to simulate in this way.

Weinberg & Katz (2002) included coefficients of odd (l, m) and hence their simulations were vulnerable to artificial effects due to off-centring. Sellwood (2003) could reproduce their results, but if he suppressed the coefficients with odd (l, m), the results were completely altered in that more than hundred instead of a few bar rotations were required to remove the density cusp. Sellwood also pointed to a previous study by White (1983) which reported that the $l = 1$ term can cause numerical artifacts. Thus, apparently, the simplified bar-halo model of Weinberg & Katz undergoes a non-reflection symmetric evolution. However, owing to the problems inherent to the use of spherical harmonics, it is unclear from the studies of Weinberg & Katz and Sellwood (2003) whether this evolution is an artifact of their algorithm (i.e. the usage of spherical harmonics) or not.

In an effort to resolve this question we performed similar simulations ourselves with a different type of N-body code, which does not rely on an expansion in spherical harmonics and hence avoids these problems. Technical details of the models used, and the N-body code are given in §2, our results are presented in §3. We discuss our results and draw conclusions in §4

2 MODELLING

For the majority of our simulations we model the halo as an isotropic spherical Hernquist (1990) model, which has density

$$\rho(r) = \frac{M_{\rm halo}\, r_{\rm s}}{2\pi r (r_{\rm s} + r)^3} \tag{2}$$

with $M_{\rm halo}$ and $r_{\rm s}$ the total mass and scale radius, respectively. This profile has the same 'cuspy' behaviour as the NFW profile (1) in the limit $r \to 0$, but has the virtue of having less mass in the outer regions of the halo. This means that a simulation with the same particle number will have greater resolution in the cusp. We introduce the bar as an external potential applied to the N-body simulation. Only the quadrupole moment of the bar is included in the force calculation, since the monopole term would have the effect of adding mass at the centre of the halo, altering the equilibrium, and higher order terms are far weaker, having little effect on the evolution, and are ignored for simplicity. A convenient fitting formula, which behaves properly as a quadrupole for both $r \to 0$ and $r \to \infty$ is provided by Hernquist & Weinberg (1992):

$$\Phi_{\rm bar} = -\frac{G M_{\rm bar}}{a} \frac{\alpha r_*^2}{(\beta^\gamma + r_*^\gamma)^{5/\gamma}} \sin^2\theta \cos 2(\varphi - \Omega_{\rm p} t). \tag{3}$$

Here, $r_* = r/a$ with a the semi-major axis of the bar, r, θ, and φ are the usual spherical polar coordinates, and $M_{\rm bar}$ and $\Omega_{\rm p}$ the mass and pattern speed of the bar, respectively. α, β and γ are dimensionless parameters determined by best fit to the chosen bar density profile and shape. The bar is 'turned on' adiabatically over ~ 10 rotation periods to minimise transient effects.

In the majority of cases we follow Hernquist & Weinberg (1992) and Sellwood (2003) and model the bar as an $n = 2$ Ferrers (1877) bar with axis ratio $1 : 0.5 : 0.1$. This is fitted by the parameters $\alpha \simeq 0.1404$, $\beta \simeq 0.4372$ and $\gamma = 2$ (while an incorrect version of this fitting formula is reproduced by Sellwood (2003), the correct model was used in his simulations, Sellwood, private communication).

The simulations of Weinberg & Katz (2002) were of a NFW density profile halo (1), truncated at large radii (as the NFW model has infinite mass, if considered for $r \to \infty$). The bar density profile used was that of a homogeneous ellipsoid of axis ratio $1 : 0.5 : 0.05$. This is well fitted by the same fitting formula used for the n=2 Ferrers bar (3), with the parameters $\alpha \simeq 0.1227$, $\beta \simeq 0.6288$ and $\gamma = 5.314$. In Section 3.2 we present simulations with the same parameters as Weinberg & Katz (2002) in an effort to directly compare our simulations with theirs. For this we used a truncated NFW halo which we defined as having the density profile

$$\rho(r) = \frac{\rho_{\rm c}}{(r/r_{\rm s})(1 + r/r_{\rm s})^2} {\rm sech}(r/10 r_{\rm s}) \tag{4}$$

2.1 Technical details

We generate the initial positions and velocities from the density (2) and the isotropic distribution function. In the case of the Hernquist halo this is known (Hernquist 1990), while in the case of the truncated NFW halo it can be found numerically using Eddington's 1916 formula. Quasi-random numbers were employed in order to suppress Poisson noise. The N-body simulations were performed using the publicly available N-body code gyrfalcON, which is based on Dehnen's (2000; 2002) force solver falcON, a tree code with mutual cell-cell interactions and complexity $O(N)$. The performance of the code is comparable to that of the spherical-harmonic based so-called SCF method

(Hernquist & Ostriker 1992; Weinberg 1999) with terms up to $n, l = 8$ included.

For the Hernquist halo we used units of time, mass, and length such that $G \equiv 1$, $r_s \equiv 11$ and $M_{\rm halo} \equiv 1$. For the truncated NFW halo we used units such that $G \equiv 1$, $r_s \equiv 1$, and $v_{\rm circ,max} \equiv 1$ The equations of motion were integrated using the familiar leap-frog integrator with minimum time step 2^{-7} and a block-step scheme allowing steps up to four times larger. Individual particle time steps were adjusted in an (almost) time-symmetric fashion such that on average

$$\tau_i = \min\left\{\frac{0.01}{|\boldsymbol{a}_i|}, \frac{0.01}{|\Phi_i|}\right\} \tag{5}$$

with Φ_i and $\boldsymbol{a}_i$ the gravitational potential and acceleration of the ith body. A fiducial simulation with $N = 3 \times 10^5$ and no imposed bar conserved energy to within 0.2% over 1500 time units corresponding to ∼120 bar rotations.

Throughout this paper lengths will be quoted in terms of halo scale lengths .

3 RESULTS

Initial simulations of a Hernquist model halo used $N = 300\,000$ and a bar of length (semi-major axis) $a = 0.7$ and mass 30% of the halo mass interior to $r = a$, as it was for all simulations in this halo type. The bar rotates with a fixed pattern speed with co-rotation at r_s, in this experiment and all others. These experiments showed a rapid change in the 1% Lagrange radius (the radius within which 1% of the total mass of the halo is contained, Fig. 1). This only demonstrates that the density at the *origin* was reduced by the action of the bar, which is not necessarily the density peak of the halo. The spherically averaged density profile (Fig. 2) seems to show the formation of a core after just 8 bar rotations. Neither of these measures take into account any possible change in the position of the centre of the distribution. Similar simulations with N ranging from 10^4 to 10^6 showed essentially the same behaviour. This is in agreement with the apparent rapid evolution seen in simulations including the $l = 1$ term by Sellwood (2003), though the timescale is slightly longer. It is similar to the evolution observed by Weinberg & Katz (2002), though the halo model is different (see Section 3.2).

3.1 Unstable evolution

This reduction in density is, however, not demonstrative of the creation of a cored density profile. Simply plotting the particle positions in the *x*-*y* plane (Fig. 3) shows that within a few bar rotations the densest part of the halo is no longer at the origin. This creates the appearance of a cored density profile if analysis is performed with respect to the origin. This effect occurs even if the initial distribution of bodies is made exactly symmetrical initially (for each body at $\boldsymbol{x}, \boldsymbol{v}$ there is another one at $-\boldsymbol{x}, -\boldsymbol{v}$).

This off-centring means that these simulation results are invalid. In this simple model, the bar's centre is fixed to the origin and does not (is not allowed to) react to the off-centring of the halo. This leads to a wildly unphysical interaction between the bar and the halo which rapidly transports energy and angular momentum to the halo, and invalidates all results found this way. We strongly suspect that the rapid evolution reported by Weinberg & Katz (2002) and its $l = 1$ dependence seen by Sellwood (2003) are actually due to this off-centring. Since this effect is reproduced in our simulations, it is clear that it is a real instability of the simplified bar-halo

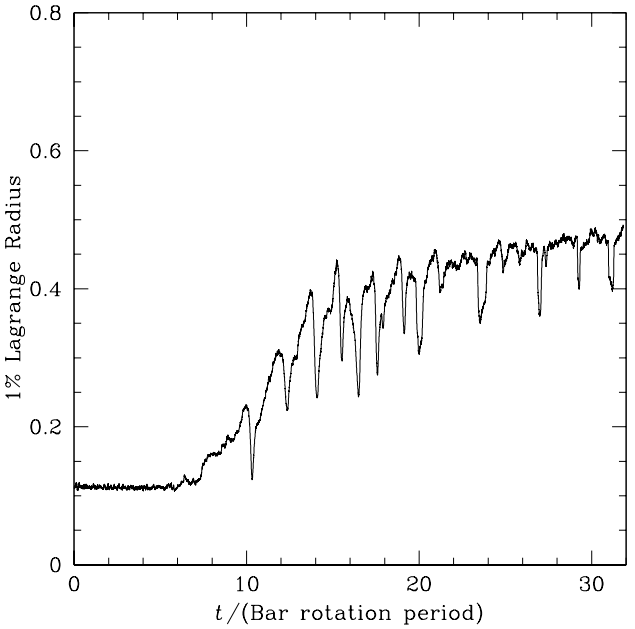

Figure 1. Time evolution of the 1% Lagrange radius in flawed simulation.

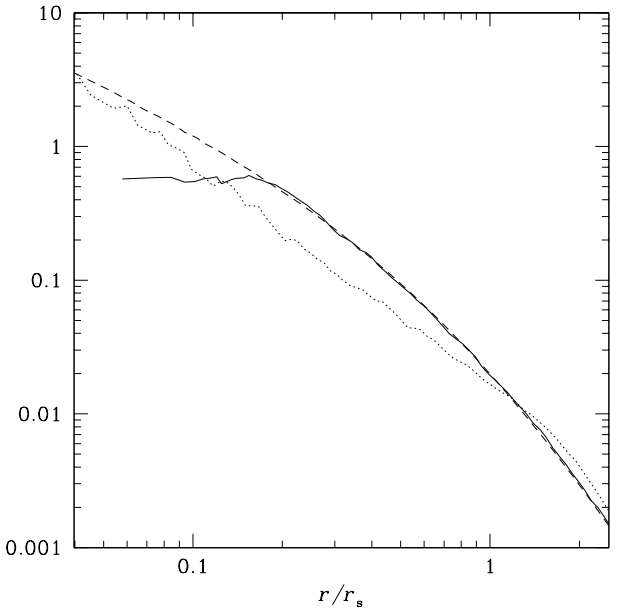

Figure 2. Spherically averaged density profile (inner part) for the same simulation as in Fig. 1. Shown are the initial profile (*dashed*); and the profile after 8 bar rotations, considered about the original centre (*solid*), or about the centre of the cusp (*dotted*). The profile appears to be cored after 8 bar rotation times but this is because the implicit assumption of conserved (or at least approximately conserved) spherical symmetry is incorrect, see Fig. 3. The profile considered about the centre of the cusp shows that the cusp is as strong as ever, but the force applied by the bar has become wildly unphysical, so this is result is, in any case, insignificant.

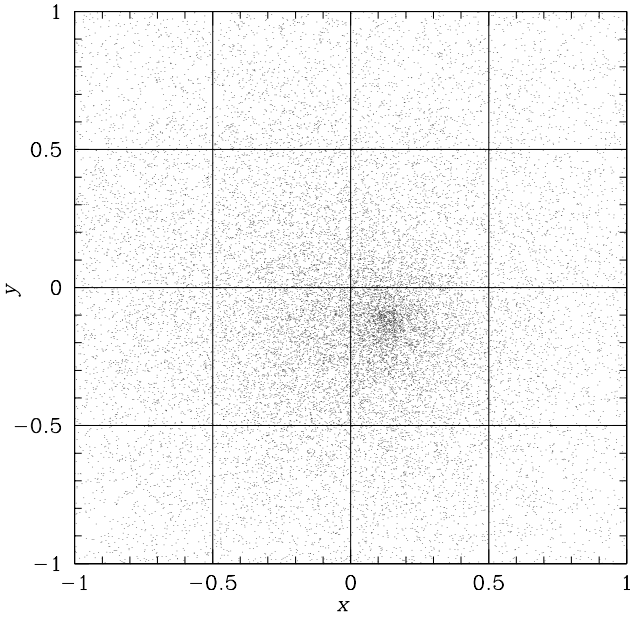

Figure 3. Positions in the *x*-*y* plane of bodies with $|z| < 1$ after 8 bar rotations. The plot shows that the centre of the distribution has shifted from the origin, thus invalidating the simulation setup.

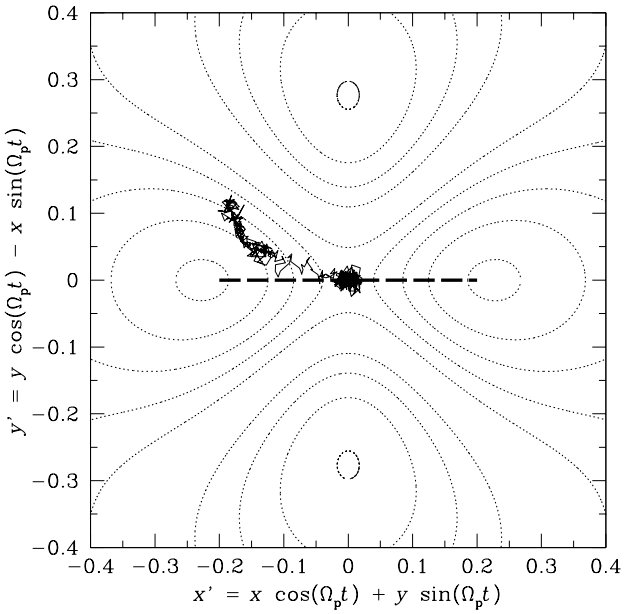

Figure 4. Motion of the density centre in the plane co-rotating with the bar during the first 11 bar rotations (*solid line*) for the same simulation as in previous Figures. The *thick dashed line* indicates the orientation of the bar, which rotates anticlockwise. Contours of the sum of the effective bar quadrupole potential in this frame and an approximation for the halo-bulk potential (halo without cusp, using a $\gamma = 0$ Dehnen (1993) model) are shown as *dotted* curves. Stationary points perpendicular to the bar are maxima, origin is a saddle point, other stationary points along the bar axis are minima.

system investigated, and is not entirely due to an artifact of the spherical harmonic approach noted by Sellwood (2005).

The initial conditions with the applied quadrupole potential are entirely point symmetric about the origin. However they are unstable to motion of the cusp away from the centre of the bar. This occurs even when the initial particle distribution is defined to be exactly symmetric, because slight asymmetries caused by numerical truncation errors break the imposed symmetry.

The cause of this instability can be understood by considering the external quadrupole potential applied to the *N*-body system. Figure 4 shows the position of the central density in the frame of the rotating bar, overlaid upon a contour plot of the quadrupole potential. The cusp of the halo is initially at a saddle point of the external potential. This is unstable to a small movement of the cusp. We can think, in a simplistic picture, of the 'cusp' falling into a potential well. The restoring force due to the bulk of the halo is too weak to counter this. We also note that the cusp does not fall to the exact centre of the well, which is presumably due to the Coriolis force.

3.2 NFW halo

In an effort to re-examine the results of Weinberg & Katz (2002), we ran simulations of an NFW halo with the same parameters they used. These simulations had a short, light bar with semi-major axis a=0.5r_s; and a mass equal to 15% of the halo mass within the bar radius. Since Weinberg & Katz suggested that high numerical resolution was required to accurately simulate the resonant dynamics, we modelled the halo with particles of varying mass, with the lowest mass particles in the inner regions where the important resonant processes occur. This allows an substantial increase in the resolution of the inner regions of the NFW halo, without increasing the total particle number. We can define N_{eff}, the effective particle number, as $N_{\rm eff} = M_{\rm tot}/m_{\rm lowest}$, where $M_{\rm tot}$ is the total mass of the halo, and $m_{\rm lowest}$ is the mass of the lowest mass particles (the particles in the innermost regions of the halo). In this way we were able to improve the resolution of our simulations such that $N_{\rm eff} \simeq 5 \times N$ without loss of stability.

Experiments utilising gyrfalcON, and with the $N_{\rm eff}$ varying between 30 000 and 6 000 000 showed no significant evolution of the halo under these conditions. The bar potential was too weak to destabilise the halo and move its centre. This is in contrast to simulations with *N* between 10 000 and 4 000 000, run with the potential expansion codes of Weinberg & Katz, and Sellwood which *did* become unstable rapidly (within ~10 bar rotations). The very low *N* at which this instability is observable in the potential expansion case, and the absence of instability even in the high *N* tree code (gyrfalcON) case, indicates that this difference is not caused by particle noise drowning out the effect of the bar in the tree code case. The potential expansion approach is clearly more susceptible to the instability of the system than a tree code.

It should be noted that there are two separate instabilities. The genuine instability of the artificial bar-halo system was responsible for the shift of the cusp away from the origin in the simulations with the Hernquist halo. In the NFW case the bar is too weak to destabilise the halo when gyrfalcON is used, but using a potential expansion approach exacerbates the problem because of the odd (l, m) instability referred to by Sellwood.

3.3 Preventing instability

3.3.1 Forcing symmetry

In our simplified model, both the halo and the bar are entirely point symmetric about the origin. The particle distribution would remain so for all time (thus preventing the instability) if it were not for trun-

cation errors in the properties of the particles as determined during the simulation. In order to investigate the situation without the confusion caused by the instability, we ran a number of simulations in which the distribution of bodies was kept point symmetric about the origin at all times. To this end we treat the bodies as pairs, and for each pair a and b, we enforce that $\boldsymbol{x}_a + \boldsymbol{x}_b = 0$ and $\boldsymbol{v}_a + \boldsymbol{v}_b = 0$ in the initial conditions and after each time step.

This is effectively the equivalent of simulations using an expansion in spherical harmonics which exclude all the terms with odd (l, m). Such experiments were carried out by Sellwood (2003).

As Figure 5 shows, the ability of a rotating bar to remove a cusp is genuine, and not reliant upon instability. Even when the simulation is completely symmetric, angular momentum transferred from the bar to the halo eventually removes the cusp. The dependence of the effect on N and bar strength are comparable to the results obtained by Sellwood (Figure 5). The major difference to note is that our results do not yet seem to converge at high N. This is likely caused by our force solver allowing stochastic jitter in the body distribution to be passed to the forces more readily than a method involving only low-order spherical harmonics does.

3.3.2 Using a more realistic bar model

An alternative method for stabilising the simulation is to allow the bar to "have mass", and thus provide a restoring force on the halo. This was achieved in our simulations by including the monopole component of the bar potential in the force calculation. The initial distribution function of the halo with the additional monopole potential can be determined using Eddington's formula. In these simulations the monopole component of the potential was included at all times, the quadrupole was added adiabatically as in all previous simulations. Any off-centring of the halo causes an artificial transfer of linear momentum from the bar to the halo, so in addition the bar was constrained to move in such a way that the linear momentum of the bar-halo system was conserved.

Figure 5 shows a comparison of the results from this approach to those from the symmetrised simulations. The movement required of the bar in order to conserve the linear momentum of the system was extremely small, and only carried the bar a distance $\sim 10^{-5} r_s$, which is several orders of magnitude smaller than the movement of the cusp seen in Figure 4. Simulations which included the monopole in the bar potential, but in which the bar was pinned to the origin produced results which were nearly indistinguishable from those with a moving bar. It is clear that the restoring force provided by inclusion of the monopole term is sufficient to prevent the growth of the instability in this case. The presence of the monopole and removal of the artificially enforced symmetry prevent the rapid "runaway" evolution seen at $t \simeq 170$ in the corresponding symmetrised simulation. However the bar still removes the cusp of the halo over approximately the same timescale in the two simulations.

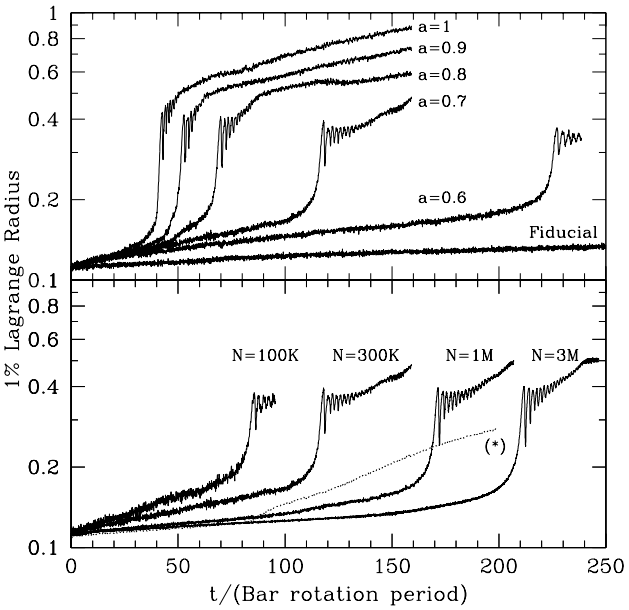

Figure 5. The 1% Lagrange radius plotted against time for many different simulations. *Top*: the effect of increasing bar size with fixed $N = 300\,000$ and enforced symmetry. Bar mass was defined as 30% of the halo mass within the bar radius for all cases. Also shown are the results of a fiducial run with $N = 300\,000$ and no imposed bar. *Bottom*: the effect of increasing resolution (particle number), for fixed bar size $a = 0.7$ and enforced symmetry also showing *(Dotted)* simulation with conserved linear momentum with same bar size, and $N = 1\,000\,000$ (*)

3.4 Angular Momentum conservation

These experiments are deliberately kept as simple as possible, which leaves them unrealistic. One major difference between the simulations described thus far and the true situation is the apparent infinite supply of angular momentum for the bar, which keeps it rotating with the same pattern speed for the entirety of the simulation, however much angular momentum has been transferred to the halo. Weinberg & Katz (2002) pointed to a "suite of simulations with a slowing bar, whose pattern speed follows from the conservation of angular momentum of the combined bar-halo system" as further evidence pointing to the effectiveness of this process in removing the cusp. However these results are tainted by the instability of the system, so we repeat the experiments with a slowing bar and the symmetrisation method to prevent instability. This is somewhat similar to experiments performed by Sellwood (2003), with the $l = 1$ spherical harmonic suppressed. Since initially the bar has zero mass, and the mass (and thus angular momentum) is increased adiabatically, angular momentum is introduced to the system by the growing bar. We calculate the angular momentum of the halo after each time step and use that to calculate the change in the pattern speed of the bar at every point, so that the total angular momentum added to the halo is no more than that of the bar at its full mass, rotating with its original pattern speed.

As Figure 6 shows, when the bar is not given an infinite supply of angular momentum, the situation is somewhat different. Essentially all the angular momentum of the bar is absorbed by the halo within 15 initial rotation periods (in fact the bar has made ten complete revolutions at that point). This absorbed angular momentum is insufficient to remove matter from the cusp to any great extent. In experiments carried out without symmetrisation, the central density did fall to approximately that seen in the experiments with a bar rotating with a constant pattern speed. This was again because the cusp of the distribution shifted from the origin.

4 CONCLUSIONS

We find that over-simplifying the interaction of a barred galaxy with a cusped CDM halo may lead to substantial over-estimation

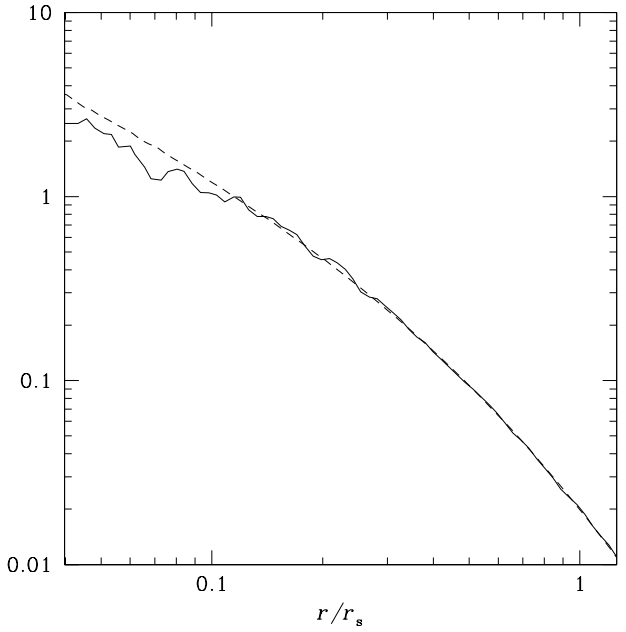

Figure 6. Density profile for a slowing bar in a $N = 300\,000$ representation of a Hernquist halo initially (*dashed*) and after 16 initial bar rotation periods (*solid*). The bar has not gone through 16 rotations, because it has decelerated, and by this point is rotating at 10% of its initial pattern speed.

of the reduction in central density. The cause is an instability of the simplified model: a slight off-centring of the CDM cusp from the origin results in a net force from the bar, which is fixed to stay centred, further driving the cusp away from the origin. The instability is implicit in the model and is not simply a result of determining the potential as a spherical harmonic expansion about the origin. It seems very likely that the rapid evolution reported by Weinberg & Katz (2002) and Sellwood (2003, when odd l terms where included in the computation of the forces) were an artifact of this instability in conjunction with averaging over spherical shells concentric with the origin (rather than the density centre).

If this artificial instability is suppressed, either by enforcing reflection symmetry w.r.t. the origin, or by including the monopole of the bar potential and conserving linear momentum, the removal of the CDM cusp is a very slow process, requiring $O(100)$ bar-rotations, i.e. a significant fraction of a Hubble time. Moreover, this simplistic model contains an additional artifact: the infinite supply of angular momentum from the ever torquing bar. If this is removed by controlling the total angular momentum, the cusp is at most slightly modified. This means that, under these conditions, the amount of angular momentum needed to remove a CDM cusp is far larger than that present in the inner parts of disk galaxies.

Of course, this work makes a large number of assumptions. The halo has been assumed to be spherically symmetric, isotropic, without substructure, isolated and initially in equilibrium. The bar was assumed to be rigid, and gas physics and bar-disk interaction were neglected. These are the same assumptions made by the paper that proposed this mechanism (Weinberg & Katz 2002). These simulations cannot tell the whole story, but they do provide an insight into the fundamental physical mechanism.

We conclude that, contrary to the original proposal, these simulations suggest that angular momentum (and energy) transport from a disk-bar is not an effective way to destroy CDM cusps, in agreement with studies using less simplistic models (Valenzuela & Klypin 2003; Athanassoula 2004). If galactic scale CDM halos truly are cored, it seems that some other process is responsible.

ACKNOWLEDGEMENT

The authors would like to thank their referee, Kelly Holley-Bockelmann, for her constructive suggestions. PJM acknowledges the support of the UK Particle Physics and Astronomy Research Council (PPARC) through a research student fellowship. Astrophysics research at the University of Leicester is also supported through a PPARC rolling grant.

REFERENCES

Athanassoula E., 2004, in IAU Symposium Vol. 220, Bars and the connection between dark and visible matter. p. 255
Barnes J., Hut P., 1986, Nature, 324, 446
Binney J., Gerhard O., Silk J., 2001, MNRAS, 321, 471
Binney J. J., Evans N. W., 2001, MNRAS, 327, L27
Blais-Ouellette S., Amram P., Carignan C., 2001, AJ, 121, 1952
Blumenthal G. R., Faber S. M., Flores R., Primack J. R., 1986, ApJ, 301, 27
Bode P., Ostriker J. P., Turok N., 2001, ApJ, 556, 93
Côté S., Carignan C., Freeman K. C., 2000, AJ, 120, 3027
Colín P., Avila-Reese V., Valenzuela O., 2000, ApJ, 542, 622
de Blok, W. J. G., McGaugh, S. S., & Rubin, V. C. 2001a, AJ, 122, 2396
de Blok, W. J. G., McGaugh, S. S., Bosma, A., & Rubin, V. C. 2001b, ApJl, 552, L23
Dehnen W., 1993, MNRAS, 265, 250
Dehnen W., 2000, ApJl, 536, L39
Dehnen W., 2002, J. Comp. Phys., 179, 27
Eddington A. S., 1916, MNRAS, 76, 572
El-Zant A., Shlosman I., Hoffman Y., 2001, ApJ, 560, 636
Ferrers N. M., 1877, Q. J. Pure Appl. Math., 14, 1
Gentile G., Salucci P., Klein U., Vergani D., Kalberla P., 2004, MNRAS, 351, 903
Hayashi E., Navarro J. F., Power C., Jenkins A. R., Frenk C. S., White S. D. M., Springel V., Stadel J., Quinn T. R., 2004, MNRAS, 355, 794
Hernquist L., 1990, ApJ, 356, 359
Hernquist L., Ostriker J. P., 1992, ApJ, 386, 375
Hernquist L., Weinberg M. D., 1992, ApJ, 400, 80
Holley-Bockelmann K., Weinberg M. D., Katz N., 2003 astro-ph/0306374
Kaplinghat M., Knox L., Turner M. S., 2000, Physical Review Letters, 85, 3335
Moore B., Governato F., Quinn T., Stadel J., Lake G., 1998, ApJl, 499, L5+
Navarro J. F., Frenk C. S., White S. D. M., 1996, ApJ, 462, 563
Power C., Navarro J. F., Jenkins A., Frenk C. S., White S. D. M., Springel V., Stadel J., Quinn T., 2003, MNRAS, 338, 14
Salucci P., Walter F., Borriello A., 2003, Aap, 409, 53
Sellwood J. A., 2003, ApJ, 587, 638
Sellwood J. A., 2005, ApJ, submitted (astro-ph/0407533)
Spergel D. N., Steinhardt P. J., 2000, Physical Review Letters, 84, 3760
Swaters R. A., Madore B. F., van den Bosch F. C., Balcells M., 2003, ApJ, 583, 732

Trott C. M., Webster R. L., 2002, MNRAS, 334, 621
Valenzuela O., Klypin A., 2003, MNRAS, 345, 406
van den Bosch F. C., Swaters R. A., 2001, MNRAS, 325, 1017
Weinberg M. D., 2004, astro-ph/0404169
Weinberg M. D., 1999, AJ, 117, 629
Weinberg M. D., Katz N., 2002, ApJ, 580, 627
White S. D. M., 1983, ApJ, 274, 53